Bioactive Materials 28 (2023) 376–385

Contents lists available at ScienceDirect

Bioactive Materials

journal homepage: www.keaipublishing.com/en/journals/bioactive-materials

Reduction-responsive nucleic acid nanocarrier-mediated miR-22 inhibition of PI3K/AKT pathway for the treatment of patient-derived tumor xenograft osteosarcoma

Dafu Chen [a,1], Chengyue Lei [b,1], Weifeng Liu [c,1], Meiyu Shao [b], Meizhou Sun [b], Jianxun Guo [a], Jingjing Cao [a], Jing-Jun Nie [a], Peng Luo [a], Yuwen Luo [a], Bingran Yu [b], Renxian Wang [a,d,*], Shun Duan [b,**], Fu-Jian Xu [b,***]

[a] Laboratory of Bone Tissue Engineering, Beijing Laboratory of Biomedical Materials, National Center for Orthopaedics, Beijing Research Institute of Traumatology and Orthopaedics, Beijing Jishuitan Hospital, Beijing, 100035, China
[b] State Key Laboratory of Chemical Resource Engineering, Key Lab of Biomedical Materials of Natural Macromolecules (Beijing University of Chemical Technology), Ministry of Education, Beijing Laboratory of Biomedical Materials, Beijing University of Chemical Technology, Beijing, 100029, China
[c] Department of Orthopaedic Oncology Surgery, Beijing Jishuitan Hospital, Peking University, Beijing, 100035, China
[d] JST Sarcopenia Research Centre, Beijing Research Institute of Traumatology and Orthopaedics, Beijing Jishuitan Hospital, Beijing, 100035, China

ARTICLE INFO

Keywords:
Nucleic acid delivery
Nanoparticle
Gene therapy
Osteosarcoma
Responsive
Patient-Derived Xenograft (PDX)

ABSTRACT

miRNAs are important regulators of gene expression and play key roles in the development of cancer, including osteosarcoma. During the development of osteosarcoma, the expression of miR-22 is significantly down-regulated, making miR-22 as a promising therapeutic target against osteosarcoma. To design and fabricate efficient delivery carriers of miR-22 into osteosarcoma cells, a hydroxyl-rich reduction-responsive cationic polymeric nanoparticle, TGIC-CA (TC), was developed in this work, which also enhanced the therapeutic effects of Volasertib on osteosarcoma. TC was prepared by the ring-opening reaction between amino and epoxy groups by one-pot method, which had the good complexing ability with nucleic acids, reduction-responsive degradability and gene transfection performance. TC/miR-22 combined with volasertib could inhibit proliferation, migration and promote apoptosis of osteosarcoma cells *in vitro*. The anti-tumor mechanisms were revealed as TC/miR-22 and volasertib could inhibit the PI3K/Akt signaling pathway synergistically. Furthermore, this strategy showed outstanding tumor suppression performance in animal models of orthotopic osteosarcoma, especially in patient-derived chemo-resistant and chemo-intolerant patient-derived xenograft (PDX) models, which reduced the risk of tumor lung metastasis and overcame drug resistance. Therefore, it has great potential for efficient treatment of metastasis and drug resistance of osteosarcoma by the strategy of localized, sustained delivery of miR-22 using the cationic nanocarriers combined with non-traditional chemotherapy drugs.

1. Introduction

Osteosarcoma (OS) is the most common primary malignant tumor of bone, which has a peak incidence in adolescents and young adults coinciding with the pubertal growth spurt. Overall survival rates of osteosarcoma have stagnated in the past four decades and there is an urgent need to identify novel targets and develop more effective treatment strategies [1–3]. The current chemotherapy combined with surgery treatment has improved the five-year survival rates to 60%–70% [4]. Moreover, OS is highly invasive and prone to metastasize to the lung and other bones, leading to an overall five-year survival rate of less than 20%. Furthermore, the current treatment model has high risk of causing

Peer review under responsibility of KeAi Communications Co., Ltd.
* Corresponding author. Laboratory of Bone Tissue Engineering, Beijing Laboratory of Biomedical Materials, National Center for Orthopaedics, Beijing Research Institute of Traumatology and Orthopaedics, Beijing Jishuitan Hospital, Beijing, 100035, China.
** Corresponding author.
*** Corresponding author.
E-mail addresses: wrxpumc@126.com (R. Wang), duanshun@mail.buct.edu.cn (S. Duan), xufj@mail.buct.edu.cn (F.-J. Xu).
[1] These authors contributed equally to this work.

https://doi.org/10.1016/j.bioactmat.2023.05.012
Received 21 April 2023; Received in revised form 10 May 2023; Accepted 11 May 2023
Available online 12 June 2023

drug resistance problems [5]. Additionally, because the early symptoms of OS are similar to those of growing pains, late diagnosis often occurs, further complicating treatment. Therefore, developing efficiently therapeutic strategies against osteosarcoma, such as gene therapy and chemical therapy, remains challenging.

miRNAs are small, endogenous, non-coding RNAs ranging from 18 to 25 nucleotides in length. Typically, miRNAs inhibit the translation of target genes or cause degradation of target genes by binding to the 3′ untranslated region (UTR) of the target gene on messenger RNAs (mRNAs) [6,7]. The human genome contains more than 1000 miRNAs, and each miRNA may regulate hundreds of genes under different conditions [8,9]. Consistently , miRNAs also play an important role in the occurrence, progression, and metastasis of OS [10]. For example, the expression level of miR-22 in the plasma of OS patients was significantly lower than that of healthy volunteers. Furthermore, the expression level of miR-22 was also correlated with tumor size, clinical stage, distant tumor metastasis, and adverse effects of preoperative chemotherapy (such as chemotherapy resistance) in OS patients [11]. Additionally, miR-22 inhibits autophagy through the PI3K/AKT signal pathway, thereby promoting the sensitivity of cancer cells to the chemotherapeutic drug, cisplatin [12,13]. miR-22 also inhibits proliferation and migration of OS cells by targeting HMGB1 and therefore inhibiting HMGB1-mediated autophagy [14]. Moreover, miR-22 promotes apoptosis of OS cells by inducing cell cycle arrest [15]. Therefore, miR-22 is not only promising as a diagnostic marker for OS, but also has great potential as a therapeutic target against OS.

To introduce therapeutic nucleic acid into target cells, a delivery carrier is an essential factor. Cationic polymers, such as polyethyleneimine (PEI) and poly(L-lysine) (PLL), have attracted attention of researchers in the field of gene carriers due to their advantages of simple preparation, flexible structural design, and low immunogenicity [16–20]. One-pot ring-opening reactions using amino groups and epoxy groups have been widely used to prepare efficient and safe cationic polymeric carriers. Based on the ring-opening reaction of amino and epoxy groups, the polyhydroxy cationic polymer was synthesized, which showed very low cytotoxicity and high transfection efficiency (1000 times higher than that of PEI) [21].

To improve the delivery efficiency, responsiveness to tumor cells is also an essential property. The intracellular concentration of glutathione (GSH) is 1000 times higher than the extracellular concentration. Furthermore, the intracellular GSH concentration of tumor cells is 7–10 times higher than that of normal cells due to exuberant metabolism [22,23]. Therefore, reduction-responsive disulfide bonds can be introduced in the cationic polymer in response to high concentrations of GSH inside tumor cells. Under the action of high concentration of GSH inside tumor cells, the disulfide bonds will be broken, leading to degradation of the cationic polymer and rapid release of the loaded nucleic acids. Therefore, such chemical structure can improve the transfection efficiency and reduce cytotoxicity [24–26]. For example, GSH-responsive silica nanocapsules could enhance the CRISPR therapeutic effects [27]. GSH-responsive silica nanoparticles showed outstanding performances in miRNA delivery for treating multidrug-resistant cancers [28]. GSH-responsive nanogels have been reported for efficient combination cancer therapy [29].

In this work, a reduction-responsive polyhydroxy cationic gene nanocarrier (TC) was synthesized by a one-pot method (Scheme 1). By a facile synthesis method, nanoparticles with high transfection efficiency and responsiveness to tumor cells were fabricated to deliver miRNA for osteosarcoma therapy. The responsive degradation performance of TC was tested by agarose gel electrophoresis. Transfection assays were performed in Saos-2 cells and MC3T3-E1 cells, and the reduction responsiveness of TC was further reflected by comparing the transfection efficiencies between the two cell lines. Furthermore, qRT-PCR and *in vitro* anti-tumor experiments were used to detect the transfection efficiency of TC-mediated miR-22. Finally, the tumor growth inhibition abilities of TC mediated miR-22 were evaluated in orthotopic OS animal models, patient-derived xenograft (PDX) models and drug-resistant PDX models, especially when combined with an anticancer drug, Volasertib. This work provides a promising strategy of design and fabrication of efficient gene delivery nanoplatforms for osteosarcoma therapy.

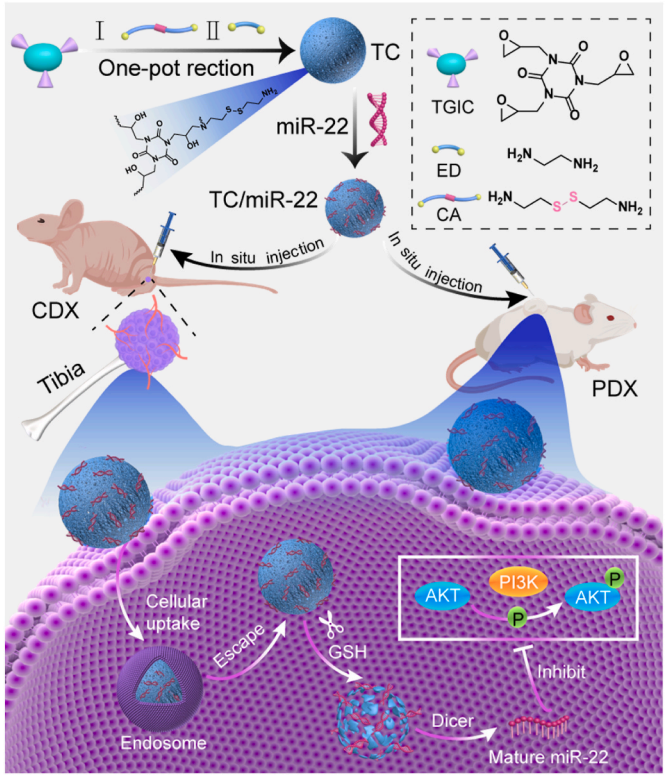

Scheme 1. Schematic illustration of the preparation process of reduction-responsive cationic polymer TC and its application for mediating miR-22 in the treatment of osteosarcoma.

2. Results and discussion

2.1. Physical, chemical and biophysical properties

The synthesis process and biologic application of TC was shown in Scheme 1, and the detailed synthetic route of TC and TH (a control group without disulfide bonds) are shown in Fig. S1of the Supporting Information. Firstly, TC or TH was prepared via a one-pot epoxy ring-opening reaction of 1,3,5-triglycidyl isocyanurate (TGIC) with cystamine (CA) or 1,6-hexanediamine (HMDA), respectively. Excessive ethylenediamine (ED) was added at the end of the reaction to consume the residual epoxy groups. Typical 1H NMR spectra confirmed the successful synthesis of TC and TH (Fig. S2, Supporting Information). The results of element analysis of TC and TH demonstrated the introduction of sulfur into TC (Table S1, Supporting Information). TH was a soluble polymer, and its molecular weights and polydispersity indexes (PDI) of TH were measured by GPC (Table S2 of Supporting Information). The morphology of TC in the aqueous solution was observed as spherical nanoparticles with a diameter of about 150 nm (Fig. 1a). To investigate the formation of TC nanoparticles, the morphology of TC before dialysis was observed (Fig. S3, Supporting Information). The TEM image showed that the nanoparticle morphology was formed after the reaction of TGIC and CA in DMSO. Therefore, TC nanoparticles might be formed by crosslinking of the rearrangement reaction of disulfide bonds [30,31].

The complexing abilities of TC and TH with nucleic acids were assessed by agarose gel electrophoresis. Both TC and TH could efficiently complex with miRNA at the weight ratio of 1.5 and above (Fig. 1b). Additionally, TC and TH could also condense DNA. As shown

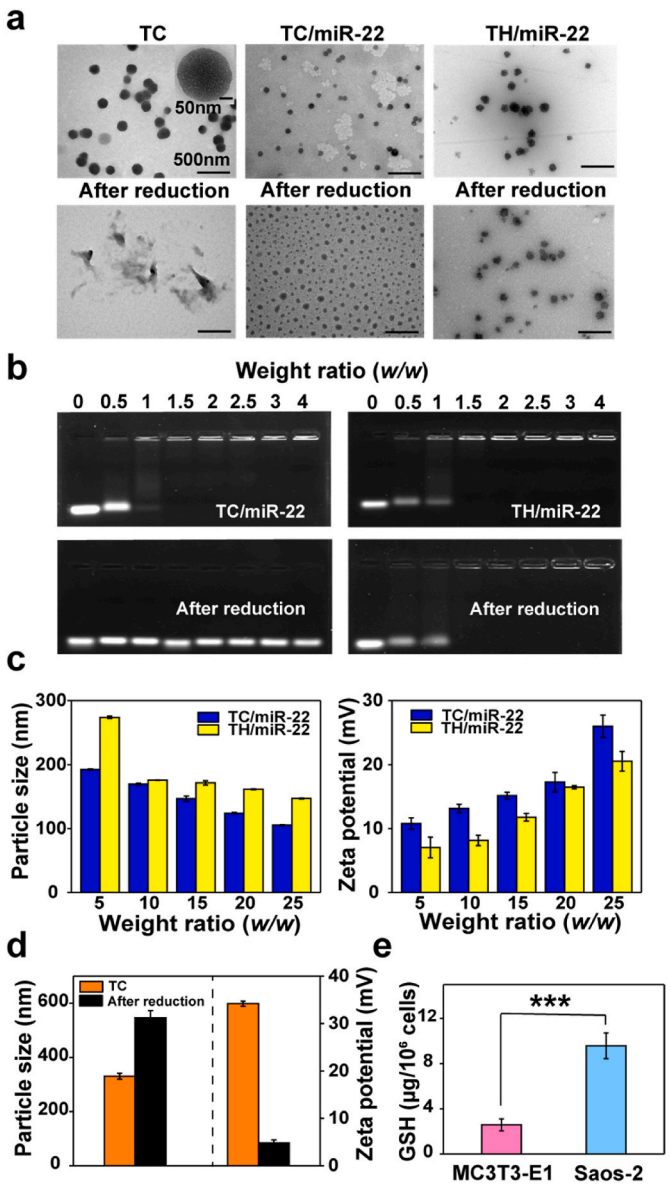

Fig. 1. a) TEM images of TC, TC/miRNA and TH/miRNA complexes and their responsiveness to reduction; b) electrophoretic mobility retardation assay of TC/miRNA and TH/miRNA complexes before and after reduction at various weight ratios; c) particle sizes and zeta potentials of TC/miRNA and TH/miRNA at different mass ratios; d) particle size and zeta-potential of TC and TC + DTT; e) GSH contents in Saos-2 cells compared with MC3T3-E1 cells. Each bar represents the mean ± SD of three independent observations. (*p < 0.05, **p < 0.01, ***p < 0.001, and ****p < 0.0001).

in Fig. S4a, they complexed with pDNA within the weight ratios of 0.5–1 (Fig. S4a, Supporting Information). Then, the particle sizes and zeta potentials of TC/miRNA and TH/miRNA complexes at various weight ratios were measured (Fig. 1c). With the increase of weight ratio, miRNAs were more tightly condensed by polymers, leading to smaller particle sizes. The particle sizes of all complexes were around 200 nm, which facilitated endocytosis [26,32]. Zeta potentials represent the surface charges of complexes. Compared with pristine TC, TC/miRNA complexes showed lower zeta potentials due to the introduction of negatively charged miRNA. With the increase of weight ratio, the number of cationic polymers in the complexes increased, resulting in increased Zeta potentials. The positively charged complexes contributed to the affinity for negatively charged cell membranes. As for the particle sizes and zeta potentials of TC/pDNA, it showed the same regular pattern as TC/miRNA (Fig. S4b, Supporting Information).

The introduction of disulfide bonds into the molecular structure of TC was aimed at achieving responsiveness to the reductive environment present inside tumor cells (as shown in Scheme 1). To investigate the degradation behavior of TC in response to a reductive environment, dithiothreitol (DTT) was used to simulate such an environment. Upon adding DTT, the spherical shape of the TC nanoparticles was disrupted, as seen in Fig. 1a. Additionally, TC/miR-22 complexes showed a looser and smaller morphology upon treatment with DTT, while TH/miR-22 complexes were not affected. The responsiveness of TC was also confirmed by the electrophoretic mobility retardation assay results, which showed that the nucleic acid was released from TC/miR-22 complexes upon treatment with DTT, while TH/miR-22 complexes were not affected (Fig. 1b). Furthermore, the particle size and zeta potential of the TC nanoparticle were characterized by DLS (Dynamic light scattering) (Fig. 1d). The particle size of nanoparticle was about 300 nm, and the zeta potential was around 35 mV. After being reduced by DTT, the particle size increased to approximately 550 nm and the zeta potential reduced to approximately 5 mV. These results demonstrated that the TC nanoparticles were successfully synthesized, which could form complexes with miRNA and respond to the reductive environment of the high concentration of GSH inside osteosarcoma cells (Fig. 1e).

2.2. *In vitro* cytotoxicity and transfection efficiency

Good biocompatibility is a necessary property for promising nucleic acid carriers. Therefore, the cytotoxicities of TC/pDNA, TH/pDNA, TC/miRNA and TH/miRNA complexes were evaluated at various weight ratio in Saos-2 and MC3T3-E1 cells lines using the thiazolyl blue tetrazolium bromide (MTT) assay (Fig. S5a, Supporting Information). Compared with the TH/NAs groups and the gold-standard of nonviral gene carriers, branched PEI (25 kDa), at the same weight ratio and its optimal transfection condition (N/P = 10), the cytotoxicity of TC/NAs complexes were the lowest in both cell lines. However, the cytotoxicity of TH/NAs was very high. The low cytotoxicity of TC may be due to the effective degradation in cells [19,25]. In addition, the polymer has plentiful hydroxyl groups, which can shield parts of excessive harmful positive charges [33]. As for TH, the non-degradable long carbon chains may damage the cell membrane and lead to cell death. Therefore, TC was chosen for the following assays due to its good biocompatibility.

In vitro transfection performances were evaluated with a pRL-CMV reporter plasmid (pDNA) in Saos-2 (osteosarcoma cell line) and MC3T3-E1 (osteoblast cell line) cells. The optimal N/P ratio of PEI/pDNA complexes was determined as 10 in both cell lines (Fig. S5b, Supporting Information), which would be taken as a control group. The transfection efficiencies of TC/pDNA complexes at various mass ratios from 5 to 25 were examined (Fig. S5c, Supporting Information). The results of transfection efficiency showed that the optimal weight ratio of TC was 10 in Saos-2 cell line. Moreover, the transfection efficiency of TC in Saos-2 cells was significantly higher than that in MC3T3-E1 cells, while the transfection efficiencies of PEI in the two cell lines were similar. This result is due to the higher GSH concentration in Saos-2 cells (Fig. 1e), which could break disulfide bonds of TC efficiently and release the loaded pDNA more rapidly.

High endocytosis efficiency is the basis of high-performance nucleic acid delivery systems. The Saos-2 cell line was utilized to investigate the phagocytosis of TC/miRNA complexes via CLSM and flow cytometry, with the miRNA labeled with FAM and the TC labeled with Cy-5.5, and the nuclei stained with DAPI. As demonstrated in Fig. 2, the fluorescence intensity of the TC/miRNA (98.8%) group was significantly higher than that of the miRNA group (1.96%), indicating that the TC/miRNA complex is essential for successful gene therapy.

Based on the results obtained, TC demonstrated excellent reduction-responsive degradability, increased gene transfection efficiency and decreased cytotoxicity. Additionally, previous studies have demonstrated that miR-22 can induce apoptosis and inhibit metastatic

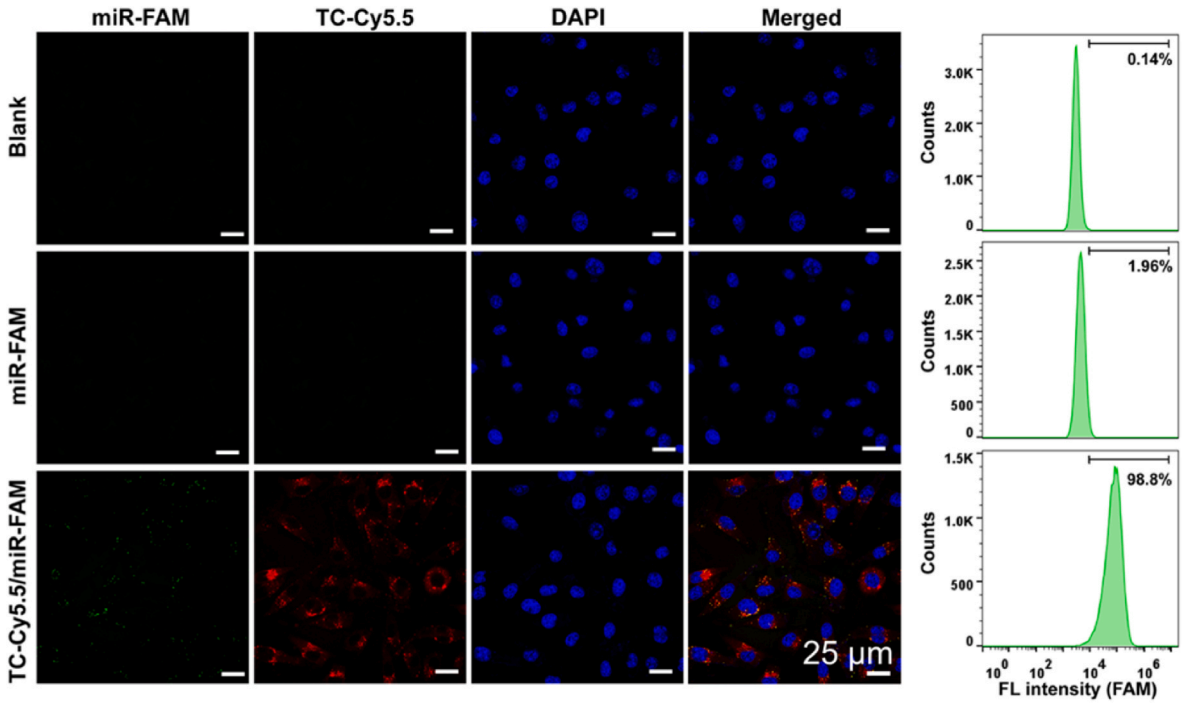

Fig. 2. Fluorescent images and their corresponding flow cytometry results of Saos-2 cells treated with miRNA and TC/miRNA complexes at the weight ratio of 10.

proliferation of OS cells [14]. Furthermore, Volasertib, a potent cell-cycle kinase inhibitor, was also identified to target PLK1 [34–36], leading to Polo arrest and apoptosis in addition to inhibiting the PI3K/AKT pathway. Consequently, the combination of miR-34a with Volasertib was proposed for enhanced Pancreatic cancer inhibition [37]. Apoptosis assays revealed an increased rate of Saos-2 cells apoptosis. At 72 h after transfection, the percentages of apoptotic Saos-2 cells treated with PBS, TC, TC/miR-NC, TC/miR-22, volasertib and TC/miR-22/Volasertib were 0.016%, 4.39%, 5.38%, 8.89%, 9.24% and 24.8%, respectively (Fig. 3a).

According to the clonal formation assays, TC/miR-NC showed more crystal violet aggregation compared with TC/miR-22, and the least aggregation was observed in the TC/miR-22/Volasertib group, demonstrating the best inhibitory effects on cell proliferation (Fig. 3b). The cell migration ability of Saos-2 cells was evaluated by wound-healing assays. The lowest percentage of cell migration was observed in the TC/miR-22/Volasertib group (Fig. 3c). In addition, the quantitative results of cell proliferation rate, apoptosis ratio and wound closure also revealed reduced cell growth and migration in the TC/miR-22/Volasertib group (Fig. 3d–f). These results demonstrated that TC/miR-22 complex with Volasertib can efficiently inhibit osteosarcoma, which have promising application for *in vivo* study.

2.3. *In vivo* antitumor performances

Since *in vitro* anti-tumor experiments had demonstrated promising therapeutic potential, further *in vivo* experiments were conducted to assess the anti-tumor efficacy of TC/miR-22 using an orthotopic tibia osteosarcoma model that was constructed using Saos-2 cells. All animal studies were conducted with approval from the Ethical Committee of Jishuitan Hospital and complying with relevant regulations. The nude mice with orthotopic tibia OS were randomly divided into five groups as PBS (control), TC/miR-NC, TC/miR-22, Volasertib and TC/miR-22/Volasertib. TC/miR-NC and TC/miR-22 were administered intratumorally while Volasertib was injected intraperitoneally. Treatment was administered every two days, and 8 days later the mice were sacrificed by cervical dislocation for subsequent analyses (Fig. 4a). Because the orthotopic OS had grown out of the bone marrow cavity of the mouse tibia, X-ray images were first taken to observe the tumor size (Fig. S6a, Supporting Information). The X-ray results revealed that the tumor volume was significantly smaller than the control and TC/miR-NC groups after TC/miR-22 treatment. The combined treatment group, TC/miR-22/Volasertib, showed the best response among all the groups, which displayed the smallest tumor size.

Finally, the tumors of these mice were harvested, photographed, and weighed (Fig. 4b–d). We observed that tumors in the control group and the TC/miR-NC group were the largest in volume and heaviest in mass, whereas tumor growth was suppressed in the TC/miR-22 group, resulting in significantly reduced volumes and masses. It was noted that the TC/miR-22/Volasertib group exhibited the most pronounced antitumor effect, having the smallest tumor volume and mass. Calculation of the tumor growth rate revealed that the combined administration of TC/miR-22 and volasertib exerted a synergistic anti-tumor effect ($S \geq 0$) [38,39]. Subsequently, the body weight changes of the mice were monitored. During the treatment process, a slight decrease in the body weight of mice in the Volasertib group was observed (Fig. S6b, Supporting Information). On the contrary, no significant weight loss was seen in other groups, indicating the good *in vivo* biocompatibility of TC.

Moreover, dissection of the experimental animals revealed that the tumors in the mice had metastasized to the lungs in the control group and the TC/miR-NC group. To confirm this result, tissue sections of the tumors and lungs were analyzed with H&E staining (Fig. 4e). The results of H&E staining showed that the nuclei of tumor cells in the control group and the TC/miR-NC group were plump and the cell structure intact. In contrast, the nuclei of tumor cells in the other three groups were shrunken. The cell morphology was altered, and the cell structure was disrupted, which exhibited obvious morphology of apoptosis. Moreover, the combination of TC/miR-22 and volasertib caused the highest degree of tumor cell damage. Notably, both the control group and the TC/miR-NC group developed tumor lung metastasis, whereas none of the treatment groups did, indicating that TC/miR-22 and Volasertib could not only inhibit tumor growth, but also effectively suppress tumor lung metastasis. Furthermore, H&E staining was performed on the major organs of the experimental animals, including heart, liver, spleen, lung, and kidney (Fig. S7, Supporting Information). The results showed that the organs were remained normal, which indicated the

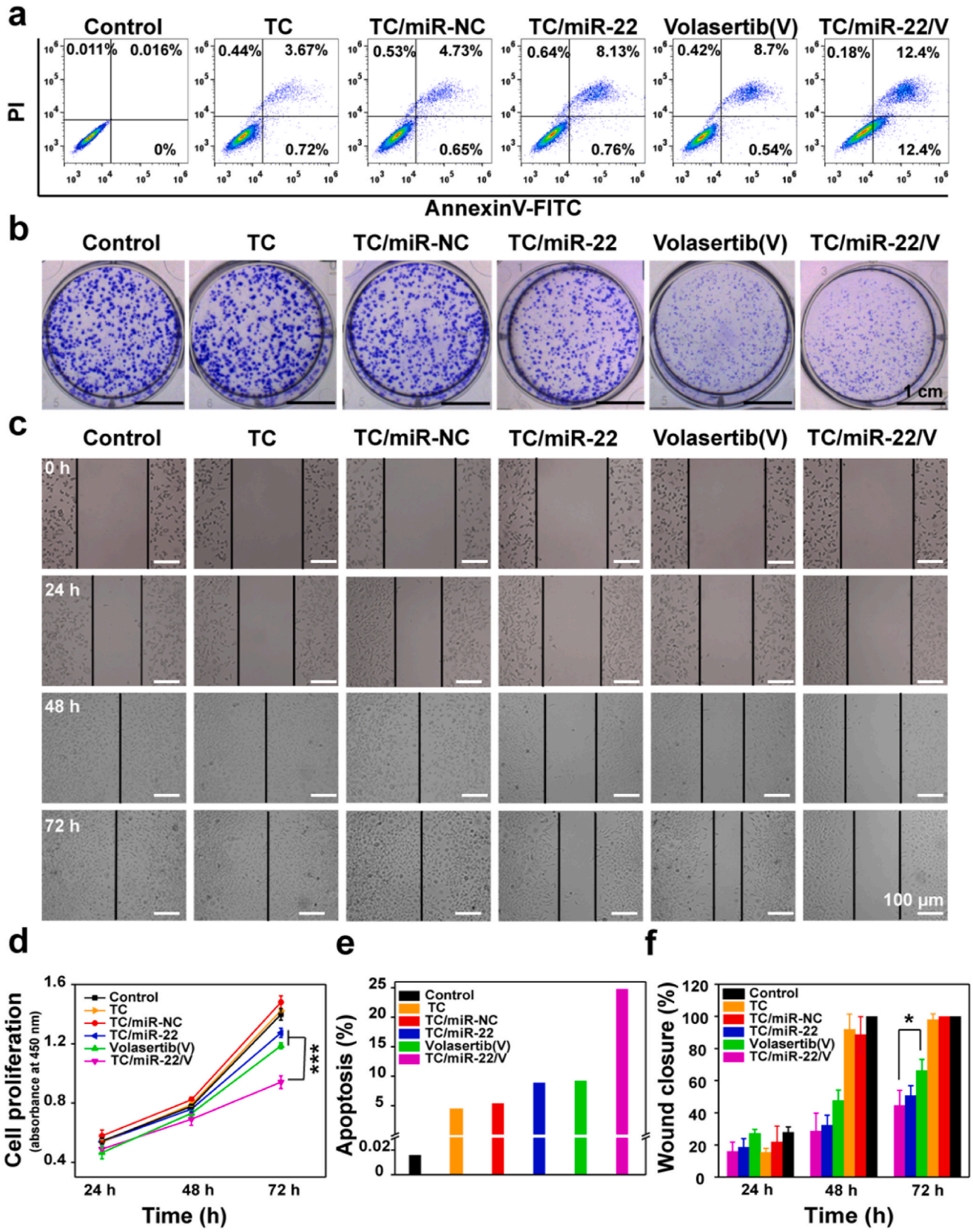

Fig. 3. a) Apoptosis induced by various treatments to Saos-2 cells; b) representative cloning formation images of Saos-2 cells at 10 d after different treatments; c) representative images of wound-healing assays in Saos-2 cells in different groups from 0 to 72 h; d) CCK-8 assay of Saos-2 cells from 24 to 72 h; e) apoptosis ratio; f) statistical analysis of wound-healing assays. Each bar represents the mean ± SD of three independent observations. (*$p < 0.05$, **$p < 0.01$, ***$p < 0.001$, and ****$p < 0.0001$).

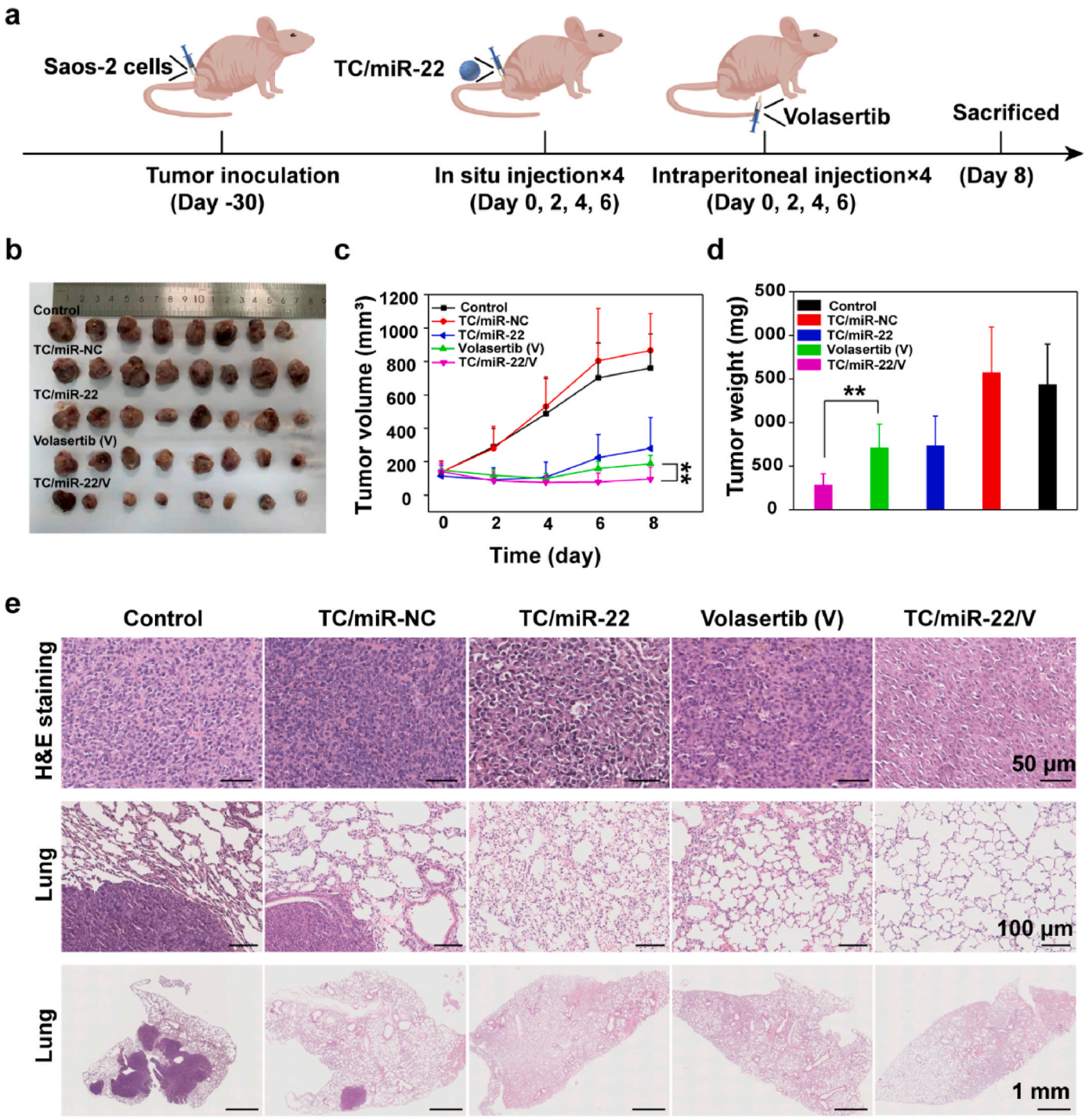

Fig. 4. a) Schematic illustration of the treatment process of animal experiments; b) images of tumors; c) the average tumor volumes; d) the average tumor weight; e) H&E staining of tumors and lungs. Each bar represents the mean ± SD of three independent observations. (*p < 0.05, **p < 0.01, ***p < 0.001, and ****p < 0.0001).

good *in vivo* biocompatibility. By these results of anti-tumor study in an orthotopic tibia osteosarcoma model, it was confirmed that TC could deliver miR-22 into osteosarcoma cell *in vivo*, exhibit outstanding anti-tumor efficacy along with Volasertib, and suppress tumor lung metastasis.

Due to the good *in vivo* anti-tumor effect in the orthotopic tibia osteosarcoma model, the therapeutic performances of TC/miR-22/Volasertib was further explored in a PDX model. The PDX samples were collected from two OS patients. This study was conducted with approval from the Ethical Committee of Jishuitan Hospital (Grant No. K2022-117-00). Because the TC/miR-22/Volasertib group achieved the best therapeutic effect in the orthotopic model, only the control group and the TC/miR-22/Volasertib group were set in the animal experiment of PDX model according to the principle of saving animals. The detailed description of PDX models is listed as follows:

PDX 1: Firstly, the P6 generation PDX 1 mouse model was constructed by using the biopsy sample from Patient 1 (Fig. 5a). Eight mice were randomly divided into 2 groups: the control group (TC/miR-NC) and the combined treatment group (TC/miR-22/Volasertib). The control group received intratumoral injection of TC/miR-NC (containing 16.5

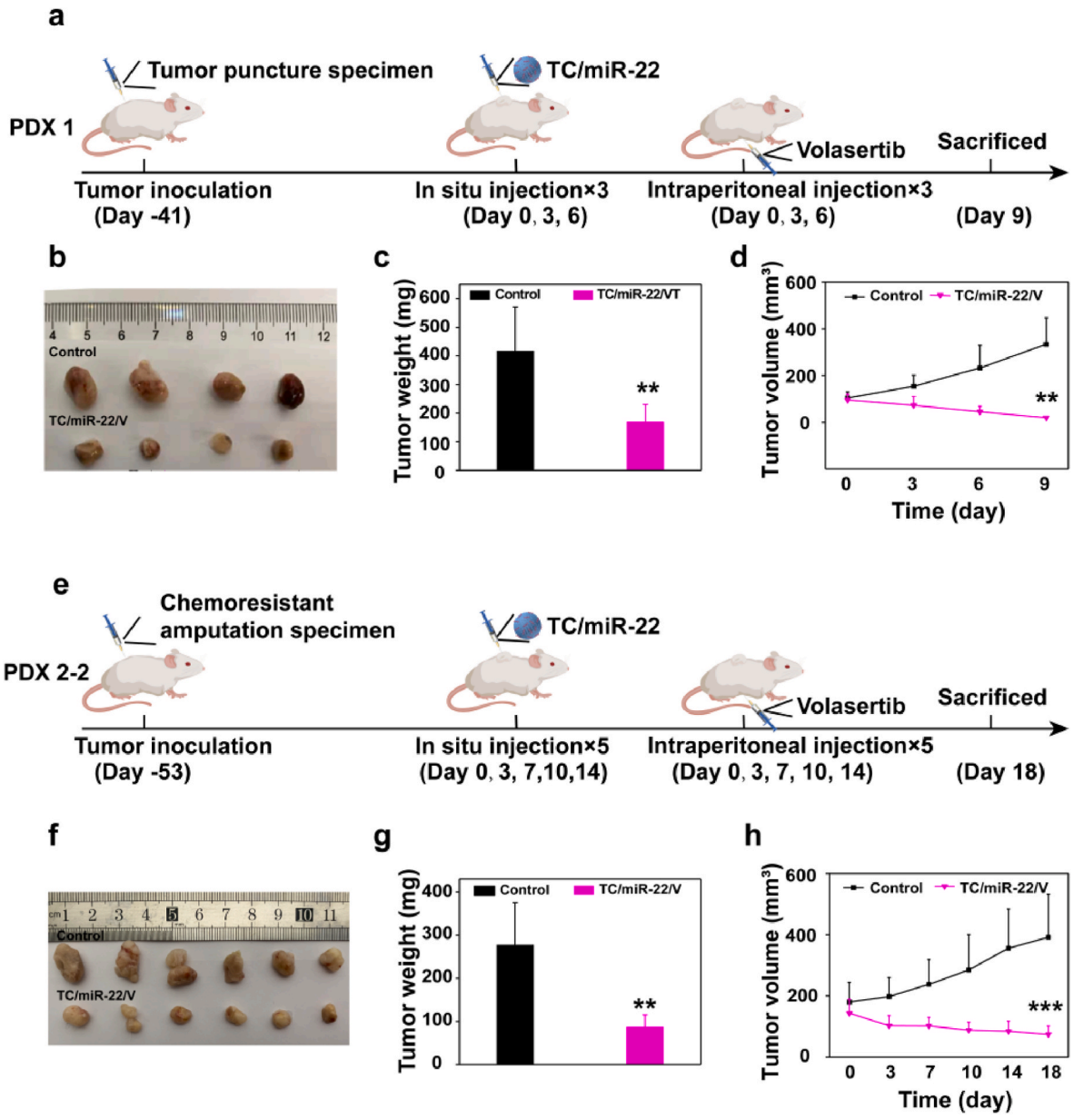

Fig. 5. a) Schematic illustration of the treatment process of osteosarcoma PDX 1 model mice; b) tumor images of PDX 1; c) average tumor weight of PDX 1; d) tumor volumes with time of PDX 1; e) schematic illustration of the treatment process of drug-resistant PDX 2-2 model mice; f) tumor images of PDX 2-2; g) average tumor weight of PDX 2-2; h) tumor volumes with time of PDX 2-2. Each bar represents the mean ± SD of three independent observations. (*$p < 0.05$, **$p < 0.01$, ***$p < 0.001$, and ****$p < 0.0001$).

μg miRNA) and intraperitoneal injection of 100 μL volasertib solvent (12.5 mg/kg). The combined treatment group received intratumoral injection of TC/miR-22 (containing 16.5 μg miRNA) and intraperitoneal injection of 100 μL volasertib solution (12.5 mg/kg). The administration was given every three days, and the mice were sacrificed on the 9th day for subsequent analysis. After 9 days of treatment, the tumor volume and mass of the mice in the TC/miR-22/Volasertib group were significantly smaller than those in the control group (Fig. 5b–d). There was no significant change in the body weight during the treatment process (Fig. S6c, Supporting Information).

PDX 2–1: Combination therapy (TC/miR-22/Volasertib) achieved favorable results in the PDX 1 model, which was established using patient biopsy samples. To further explore the therapeutic effect of this treatment on drug-resistant samples, a PDX 2-1 model was established using the amputated samples of tumor recurrence (chemotherapy drug-resistant samples) from Patient 2 (Fig. S8, Supporting Information). Twelve mice were randomly divided into the control group (TC/miR-NC) and the combined treatment group (TC/miR-22/Volasertib), and the injection method and dose were the same as PDX 1. After 9 days of treatment, the tumors in the combined treatment group were smaller than those in the control group. However, there is no statistical difference between the two groups.

PDX 2-2: To explore how to improve the efficacy on chemoresistant OS, the drug resistance PDX model (PDX 2-2) was established by using the specimens from Patient 2. While keeping the drug injection dose unchanged, the dosage of miR-22 was doubled, and the treatment time was prolonged (Fig. 5e). Twelve mice were randomly divided into two groups. The control group was injected with TC/miR-NC (including 33 μg miRNA), intraperitoneal injection of 100 μL solvent of Volasertib. In the combined treatment group, TC/miR-22 (including 33 μg miRNA) was injected into the tumor, and 100 μL of volasertib solution (12.5 mg/kg) was injected intraperitoneally. Injections were performed for 5

times, and the experimental animals were dissected on 18th day. After increasing the injection dose of TC/miR-22 and prolonging the treatment time, we found that the tumor growth in the combined treatment group stagnated. The tumor volume and weight tended to decrease in the treatment (Fig. 5h and g), while the weight of the mice did not fluctuate greatly (Fig. S6d, Supporting Information). These results show that increasing the dosage of miRNA can not only inhibit the growth of drug-resistant tumors, but also have no obvious cytotoxicity, which provides a new idea to overcome the problem of chemoresistance. Based on the results of PDX model, the *in vivo* anti-tumor efficacy was further demonstrated, especially against chemoresistant OS.

2.4. Mechanism study: regulation of p-AKT with TC/miR-22

The antitumor effects of TC/miR-22 were demonstrated both *in vivo* and *in vitro*, and its antitumor mechanism requires further exploration. To investigate this, OS tissues and adjacent tissues (normal tissues) from 12 clinical OS patients were collected, and then the relative contents of different miRNAs were analyzed by miRNA chips. As depicted in Fig. 6a, miR-22 exhibited higher expression in normal tissues compared to OS tissues, suggesting that down-regulation of miR-22 expression may be involved in the occurrence and progression of OS. Therefore, miR-22 delivery holds promise as a potential treatment strategy for OS.

The expression of miRNA was further analyzed using volcano plots using the fold change (the expression of miRNA in tumor tissues divided by the expression in normal tissues and then taking the logarithm with the base 2) as the abscissa and -Log 10 *P* value (*P* value is the significant difference value of miRNA expression in two kinds of tissues ((Fig. 6b). The results revealed that miR-22 had the smallest P value, indicating that the content of miR-22 in OS tissues and normal tissues had the most significant difference. Since miR-22 was most strongly down-regulated in OS tissues, it might have high therapeutic efficacy. To further verify this, tumor tissues and normal tissues of 25 OS patients were collected, and the content of miR-22 was detected after RNA extraction (Fig. 6c). The PCR results showed that the content of miR-22 in OS tissues of 25 patients was significantly lower than that in normal tissues, providing further evidence that miR-22 is a promising OS suppressor nucleic acid.

Based on the different expression levels of miR-22 between normal and OS tissues, the acting mechanism of TC/miR-22 was investigated. Firstly, we transfected mir22 into Saos-2 cells to overexpress it (Fig. 6d). Then, the regulation of phosphorylation of AKT protein by TC/miR-22 in the PI3K/AKT pathway in Saos-2 cells was analyzed using Western blot (Fig. 6e). The results showed that the total AKT content did not change significantly in each group after 48 h of transfection. However, compared with the TC/miR-NC group, the amount of *p*-AKT decreased in the TC/miR-22 group, and the *p*-AKT content of the Volasertib group and the combined treatment group also decreased significantly. These findings suggest that both TC/miR-22 and volasertib could effectively inhibit the phosphorylation of AKT to affect the PI3K/AKT pathway. Activated AKT can enhance cell proliferation and resist apoptosis by phosphorylating downstream factors, such as various enzymes, kinases and transcription factors [40–43]. Therefore, inhibition of the activation of AKT by TC/miR-22/Volasertib could suppress proliferation and promote cell apoptosis of osteosarcoma cells.

3. Conclusion

In this work, a disulfide bond-based polymeric nanoparticles (TC) was successfully prepared via one-pot ring-opening reactions as a biocompatible and effective miR-22 delivery system for the treatment of osteosarcoma. Due to its reduction-responsive degradability, TC possessed low cytotoxicity and demonstrated good transfection performances in osteosarcoma cells. Furthermore, TC-mediated delivery of miR-22 therapeutic system successfully induced apoptosis of OS cells and inhibited their proliferation and migration by inhibiting the PI3K/AKT pathway. *In vivo* experiments of orthotopic osteosarcoma models and PDX models further demonstrated that the TC-mediated delivery of miR-22 along with Volasertib not only inhibited tumor growth, but also reduced the risk of lung metastasis. Moreover, TC/miR-22/Volasertib also overcame the problem of chemotherapy resistance in PDX models

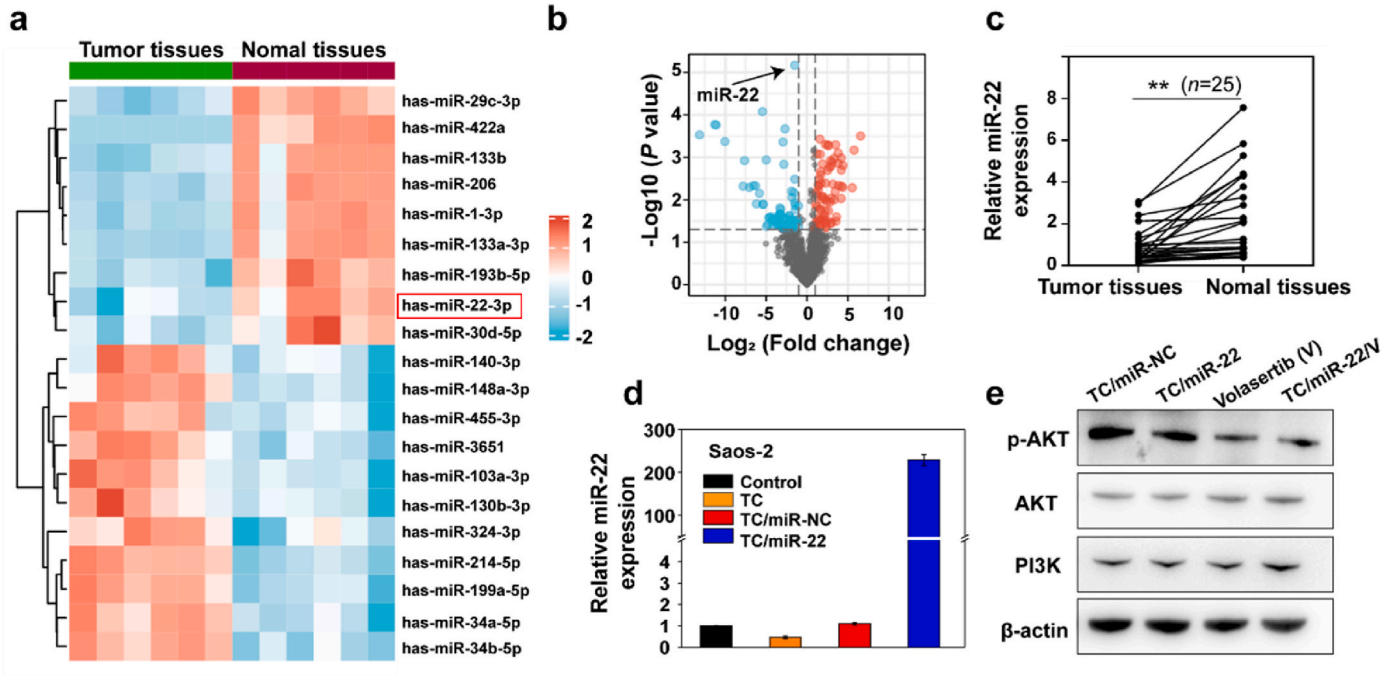

Fig. 6. a) Heatmaps showing the contents of 20 kind of miRNAs in tumor tissues in comparison with normal tissues of 12 patients with osteosarcoma (high expression was presented as red while low expression was blue); b) volcano plot showing the fold change and significant difference values of different genes in tumor tissues comprised with normal tissues; c) relative expression of miR-22 in 25 patients' tumor tissues in comparison with normal tissues; d) relative miR-22 expression of Saos-2 cells transfected with TC/miRNA complexes at the weight ratio of 10; e) relative *p*-AKT protein expression of Saos-2 cells after treatment with different groups. Each bar represents the mean ± SD of three independent observations. (*p < 0.05, **p < 0.01, ***p < 0.001, and ****p < 0.0001).

of osteosarcoma. This work provides a promising strategy in the field of gene therapy for osteosarcoma.

4. Experimental section

The detailed experimental methods were described in Supporting Information.

Conflicts of interest

There are no conflicts to declare.

CRediT authorship contribution statement

Dafu Chen: Conceptualization, Methodology, Writing – original draft, Funding acquisition. **Chengyue Lei:** Methodology, Data curation, Experimental operation, Writing – original draft, Authors reviewed the paper and approved the submitted and published versions of the paper. **Weifeng Liu:** Conceptualization, Methodology, Resources, Writing – original draft, Authors reviewed the paper and approved the submitted and published versions of the paper. **Meiyu Shao:** Data curation, experimental operation, Authors reviewed the paper and approved the submitted and published versions of the paper. **Meizhou Sun:** Authors reviewed the paper and approved the submitted and published versions of the paper. **Jianxun Guo:** Data curation, experimental operation. **Jingjing Cao:** Data curation, experimental operation, Authors reviewed the paper and approved the submitted and published versions of the paper. **Jing-Jun Nie:** Data curation, experimental operation, Funding acquisition, Authors reviewed the paper and approved the submitted and published versions of the paper. **Peng Luo:** Data curation, experimental operation, Authors reviewed the paper and approved the submitted and published versions of the paper. **Yuwen Luo:** Data curation, experimental operation, Authors reviewed the paper and approved the submitted and published versions of the paper. **Bingran Yu:** Resources, Data curation, Supervision, Authors reviewed the paper and approved the submitted and published versions of the paper. **Renxian Wang:** Conceptualization, Methodology, Supervision, Conceptualization, Writing – review & editing, Funding acquisition, Authors reviewed the paper and approved the submitted and published versions of the paper. **Shun Duan:** Conceptualization, Methodology, Supervision, Conceptualization, Writing – review & editing, Funding acquisition, Authors reviewed the paper and approved the submitted and published versions of the paper. **Fu-Jian Xu:** Conceptualization, Methodology, Supervision, Conceptualization, Writing – review & editing, Funding acquisition, Authors reviewed the paper and approved the submitted and published versions of the paper.

Declaration of competing interest

The authors declare that they have no known competing financial interests or personal relationships that could have appeared to influence the work reported in this paper.

Acknowledgement

This work was supported by National Natural Science Foundation of China (Grant Nos. 51973021, 52221006, 52173275, 51932002 and 51903013), Beijing Municipal Health Commission (BJRITO-RDP-2023, PXM 2020_026275_000002 and BMHC-2021-6), National Key Research and Development Program (Grant No. 2021YFC2400500), Beijing Jishuitan Hospital Nova Program (Grant Nos. XKXX202115 and XKXX202114) and Beijing Outstanding Young Scientist Program (Grant No. BJJWZYJH01201910010024).

Appendix A. Supplementary data

Supplementary data to this article can be found online at https://doi.org/10.1016/j.bioactmat.2023.05.012.

References

[1] R. Zheng, S. Zhang, H. Zeng, S. Wang, K. Sun, R. Chen, L. Li, W. Wei, J. He, Cancer incidence and mortality in China, 2016, J. Natl. Cancer Center 2 (1) (2022) 1–9.
[2] S.S. Bielack, B. Kempf-Bielack, G. Delling, G.U. Exner, S. Flege, K. Helmke, R. Kotz, M. Salzer-Kuntschik, M. Werner, W. Winkelmann, A. Zoubek, H. Jürgens, K. Winkler, Prognostic factors in high-grade osteosarcoma of the extremities or trunk: an analysis of 1,702 patients treated on neoadjuvant cooperative osteosarcoma study group protocols, J. Clin. Oncol. 20 (3) (2002) 776–790.
[3] F. Islami, E.M. Ward, H. Sung, K.A. Cronin, F.K.L. Tangka, R.L. Sherman, J. Zhao, R.N. Anderson, S.J. Henley, K.R. Yabroff, A. Jemal, V.B. Benard, Annual report to the nation on the status of cancer, Part 1: national cancer statistics, J. Natl. Cancer Inst. 113 (12) (2021) 1648–1669.
[4] M.S. Isakoff, S.S. Bielack, P. Meltzer, R. Gorlick, Osteosarcoma: current treatment and a collaborative pathway to success, J. Clin. Oncol. 33 (27) (2015) 3029–3035.
[5] A. Luetke, P.A. Meyers, I. Lewis, H. Juergens, Osteosarcoma treatment – where do we stand? A state-of-the-art review, Cancer Treat Rev. 40 (4) (2014) 523–532.
[6] S.P. Kabekkodu, V. Shukla, V.K. Varghese, J. D' Souza, S. Chakrabarty, K. Satyamoorthy, Clustered miRNAs and their role in biological functions and diseases, Biol. Rev. 93 (4) (2018) 1955–1986.
[7] D.P. Bartel, MicroRNAs: target recognition and regulatory functions, Cell 136 (2) (2009) 215–233.
[8] C.C. Pritchard, H.H. Cheng, M. Tewari, MicroRNA profiling: approaches and considerations, Nat. Rev. Genet. 13 (5) (2012) 358–369.
[9] M. Esteller, Non-coding RNAs in human disease, Nat. Rev. Genet. 12 (12) (2011) 861–874.
[10] L. Llobat, O. Gourbault, Role of MicroRNAs in human osteosarcoma: future perspectives, Biomedicines 9 (5) (2021) 463.
[11] Z.-B. Diao, T.-X. Sun, Y. Zong, B.-C. Lin, Y.-S. Xia, Identification of plasma microRNA-22 as a marker for the diagnosis, prognosis, and chemosensitivity prediction of osteosarcoma, J. Int. Med. Res. 48 (12) (2020), 0300060520967818.
[12] X. Yugang, C. Ming, M. Lei, Q. Yunping, H. Wenli, L. Leping, miR-22-3p enhances the chemosensitivity of gastrointestinal stromal tumor cell lines to cisplatin through PTEN/PI3K/Akt pathway, Iran. J. Allergy, Asthma Immunol. 17 (4) (2018) 318–325.
[13] C.Y. Meng, Z.Q. Zhao, R. Bai, W. Zhao, Y.X. Wang, H.Q. Xue, L. Sun, C. Sun, W. Feng, S.B. Guo, MicroRNA-22 mediates the cisplatin resistance of osteosarcoma cells by inhibiting autophagy via the PI3K/Akt/mTOR pathway, Oncol. Rep. 43 (4) (2020) 1169–1186.
[14] S. Guo, R. Bai, W. Liu, A. Zhao, Z. Zhao, Y. Wang, Y. Wang, W. Zhao, W. Wang, miR-22 inhibits osteosarcoma cell proliferation and migration by targeting HMGB1 and inhibiting HMGB1-mediated autophagy, Tumor Biol. 35 (7) (2014) 7025–7034.
[15] P. Gai, H. Sun, G. Wang, Q. Xu, X. Qi, Z. Zhang, L. Jiang, miR-22 promotes apoptosis of osteosarcoma cells via inducing cell cycle arrest, Oncol. Lett. 13 (4) (2017) 2354–2358.
[16] D.E. Olins, A.L. Olins, P.H. von Hippel, Model nucleoprotein complexes: studies on the interaction of cationic homopolypeptides with DNA, J. Mol. Biol. 24 (2) (1967) 157–176.
[17] F. Alexis, E. Pridgen, L.K. Molnar, O.C. Farokhzad, Factors affecting the clearance and biodistribution of polymeric nanoparticles, Mol. Pharm. 5 (4) (2008) 505–515.
[18] U. Lungwitz, M. Breunig, T. Blunk, A. Göpferich, Polyethylenimine-based non-viral gene delivery systems, Eur. J. Pharm. Biopharm. 60 (2) (2005) 247–266.
[19] F.-J. Xu, Versatile types of hydroxyl-rich polycationic systems via O-heterocyclic ring-opening reactions: from strategic design to nucleic acid delivery applications, Prog. Polym. Sci. 78 (2018) 56–91.
[20] M. Breunig, U. Lungwitz, R. Liebl, A. Goepferich, Breaking up the correlation between efficacy and toxicity for nonviral gene delivery, Proc. Natl. Acad. Sci. USA 104 (36) (2007) 14454–14459.
[21] S. Duan, B. Yu, C. Gao, W. Yuan, J. Ma, F.-J. Xu, A facile strategy to prepare hyperbranched hydroxyl-rich polycations for effective gene therapy, ACS Appl. Mater. Interfaces 8 (43) (2016) 29334–29342.
[22] R. Cheng, F. Feng, F. Meng, C. Deng, J. Feijen, Z. Zhong, Glutathione-responsive nano-vehicles as a promising platform for targeted intracellular drug and gene delivery, J. Contr. Release 152 (1) (2011) 2–12.
[23] W. Fan, M. Shao, J. Zhang, G. Jin, F. Liu, F.-J. Xu, A hybrid nanovector of suicide gene engineered lentivirus coated with bioreducible polyaminoglycosides for enhancing therapeutic efficacy against glioma, Adv. Funct. Mater. 29 (11) (2019), 1807104.
[24] Y. Qi, Y. Liu, B. Yu, Y. Hu, N. Zhang, Y. Zheng, M. Yang, F.-J. Xu, A lactose-derived CRISPR/Cas9 delivery system for efficient genome editing in vivo to treat orthotopic hepatocellular carcinoma, Adv. Sci. 7 (17) (2020), 2001424.
[25] Y. Huang, X. Ding, Y. Qi, B. Yu, F.-J. Xu, Reduction-responsive multifunctional hyperbranched polyaminoglycosides with excellent antibacterial activity, biocompatibility and gene transfection capability, Biomaterials 106 (2016) 134–143.
[26] J.-J. Nie, B. Qiao, S. Duan, C. Xu, B. Chen, W. Hao, B. Yu, Y. Li, J. Du, F.-J. Xu, Unlockable nanocomplexes with self-accelerating nucleic acid release for effective

staged gene therapy of cardiovascular diseases, Adv. Mater. 30 (31) (2018), 1801570.
[27] Y. Wang, X. Wang, R. Xie, J.C. Burger, Y. Tong, S. Gong, Overcoming the blood–brain barrier for gene therapy via systemic administration of GSH-responsive silica nanocapsules, Adv. Mater. 35 (6) (2023), 2208018.
[28] Peiyan Yuan, Fen Yang, Si Si Liew, Jiachang Yan, Xiao Dong, Jinfeng Wang, Shubo Du, Xin Mao, Liqian Gao, Q. Shao, Yao. Intracellular Co-delivery of native antibody and siRNA for combination therapy by using biodegradable silica nanocapsules, Biomaterials 281 (2022), 121376.
[29] Qiu-Yi Duan, Ya-Xuan Zhu, Hao-Ran Jia, Yuxin Guo, Xinping Zhang, Ruihan Gu, Chengcheng Li, Fu-Gen Wu, Platinum-coordinated dual-responsive nanogels for universal drug delivery and combination cancer therapy, Small 18 (2022), 2203260.
[30] Y. Xu, Y. Liu, X. Hu, R. Qin, H. Su, J. Li, P. Yang, The synthesis of a 2D ultra-large protein supramolecular nanofilm by chemoselective thiol–disulfide exchange and its emergent functions, Angew. Chem. Int. Ed. 59 (7) (2020) 2850–2859.
[31] M. Chen, L. Zhou, Y. Wu, X. Zhao, Y. Zhang, Rapid stress relaxation and moderate temperature of malleability enabled by the synergy of disulfide metathesis and carboxylate transesterification in epoxy vitrimers, ACS Macro Lett. 8 (3) (2019) 255–260.
[32] Y. Ren, R.-Q. Li, Y.-R. Cai, T. Xia, M. Yang, F.-J. Xu, Effective codelivery of lncRNA and pDNA by pullulan-based nanovectors for promising therapy of hepatocellular carcinoma, Adv. Funct. Mater. 26 (40) (2016) 7314–7325.
[33] B. Wang, C. He, C. Tang, C. Yin, Effects of hydrophobic and hydrophilic modifications on gene delivery of amphiphilic chitosan based nanocarriers, Biomaterials 32 (20) (2011) 4630–4638.
[34] U. Yamaguchi, K. Honda, R. Satow, E. Kobayashi, R. Nakayama, H. Ichikawa, A. Shoji, M. Shitashige, M. Masuda, A. Kawai, H. Chuman, Y. Iwamoto, S. Hirohashi, T. Yamada, Functional genome screen for therapeutic targets of osteosarcoma, Cancer Sci. 100 (12) (2009) 2268–2274.
[35] D.-W. Zheng, Y.-Q. Xue, Y. Li, J.-M. Di, J.-G. Qiu, W.-J. Zhang, J. Qiwei, Y. Yang, Y. Chen, M.-N. Wei, J.-R. Huang, K. Wang, X. Wei, Z. Shi, Volasertib suppresses the growth of human hepatocellular carcinoma in vitro and in vivo, Am. J. Cancer Res. 6 (2016) 2476–2488.
[36] B.T. Gjertsen, P. Schöffski, Discovery and development of the polo-like kinase inhibitor volasertib in cancer therapy, Leukemia 29 (1) (2015) 11–19.
[37] X. Xin, F. Lin, Q. Wang, L. Yin, R.I. Mahato, ROS-responsive polymeric micelles for triggered simultaneous delivery of PLK1 inhibitor/miR-34a and effective synergistic therapy in pancreatic cancer, ACS Appl. Mater. Interfaces 11 (16) (2019) 14647–14659.
[38] M. Hegreness, N. Shoresh, D. Damian, D. Hartl, R. Kishony, Accelerated evolution of resistance in multidrug environments, Proc. Natl. Acad. Sci. USA 105 (37) (2008) 13977–13981.
[39] X. Dai, X. Zhao, Y. Liu, B. Chen, X. Ding, N. Zhao, F.-J. Xu, Controlled synthesis and surface engineering of janus chitosan-gold nanoparticles for photoacoustic imaging-guided synergistic gene/photothermal therapy, Small 17 (11) (2021), 2006004.
[40] A. Brunet, A. Bonni, M.J. Zigmond, M.Z. Lin, P. Juo, L.S. Hu, M.J. Anderson, K. C. Arden, J. Blenis, M.E. Greenberg, Akt promotes cell survival by phosphorylating and inhibiting a forkhead transcription factor, Cell 96 (6) (1999) 857–868.
[41] I. Vivanco, C.L. Sawyers, The phosphatidylinositol 3-kinase–AKT pathway in human cancer, Nat. Rev. Cancer 2 (7) (2002) 489–501.
[42] Z.-X. Zhao, Y.-Q. Zhang, H. Sun, Z.-Q. Chen, J.-J. Chang, X. Wang, X. Wang, C. Tan, S.-J. Ni, W.-W. Weng, M. Zhang, L. Wang, D. Huang, Y. Feng, W.-Q. Sheng, M.-D. Xu, Calcipotriol abrogates cancer-associated fibroblast-derived IL-8-mediated oxaliplatin resistance in gastric cancer cells via blocking PI3K/Akt signaling, Acta Pharmacol. Sin. 44 (2022) 178–188.
[43] Q. Wang, S. Wu, Y. Gu, H. Liang, F. He, X. Wang, D. He, K. Wu, RASAL2 regulates the cell cycle and cyclin D1 expression through PI3K/AKT signaling in prostate tumorigenesis, Cell Death Discov. 8 (1) (2022) 275.